SURFACE PROPERTIES OF MAXWELL MONTES USING NEW ARECIBO DUAL-POLARIZATION RADAR DATA. S. Bhattacharyya[1], S. S. Bhiravarasu[2], G. Thangjam[1], A. K. Virkki[3], and E. G. Rivera-Valentín[4], [1]National Institute of Science Education and Research (NISER), Khurda 752050, Odisha, India (soumik.bhattacharyya@niser.ac.in), [2]Space Applications Centre (ISRO), Ahmedabad, Gujarat, India, [3]University of Helsinki, Finland, [4]Johns Hopkins University Applied Physics Laboratory, Laurel, MD.

Introduction: Numerous studies show that many of Venus's highlands have distinctly elevated values of radar reflectivity [e.g., 1] and thus low values of radar emissivity at their summits [2]. Maxwell Montes, on the eastern side of Ishtar Terra, is the highest and steepest mountain range on Venus, and has been of great interest due to the presence of complex tectonic structures as well as material properties. Unlike other highland terrain such as the Ovda Regio, the relationship between radar properties and elevation in Maxwell Montes is quite different such that it exhibits a "snow line," across which radar backscatter coefficients increase sharply (and emissivities drop sharply) with increasing elevation [3, 4].

Previous observations of Maxwell Montes using Magellan radar, emissivity, and altitude data indicated that the surface undergoes a step-like shift in the emissivity values as a function of the altitude [e.g., 3, 5], for which there is no current explanation partly due to the large altimetry and radiometry footprints. Moreover, recent ground-based Arecibo Observatory (AO) S-band radar observations revealed a region surrounding and west of the 90-km crater Cleopatra with lower same-sense circular (SC) radar echoes and circular polarization ratio (μ_C) despite increased surface reflectivity [5]. In this work, we seek to understand whether the variations in Maxwell radar echoes arise from changes in the surface reflectivity (dielectric permittivity), or are more strongly linked to changes in the surface morphology (e.g., wavelength-scale rock population, volume scattering from mantling debris).

Data and Methods: (i) AO S-band "calibrated" multi-look radar data [6]: Due to the power calibration differences between 2015 and 2017 data [6], we used the 2015 data exclusively for analysis of Maxwell features and the 2017 data for inter-comparison of Maxwell with other features (ii) Altimetry and emissivity from the Magellan global topography data records (GTDR) and global emissivity data records (GEDR), to re-verify the sharp contrast of radar properties from the Maxwell Montes (Figure 1). To understand the regional variations in radar brightness across the Maxwell Montes, we compared them to other radar-bright features (floors of the craters Audrey, Aurelia, Seymour, Faustina, Browning, Mukhina, along with Seymour impact melt flow; and lava flows associated with Sif and Gula Mons) and radar-dark features (fine-grained parabolas associated with the above listed craters) from the 2017 Arecibo data. From AO radar data of these regions, we extracted the mean values of opposite-sense circular (OC), SC and μ_C echoes for our analysis (Figures 2, 3).

Results & Discussion: As seen from Figure 1, if μ_C is considered as a proxy for radar brightness, Maxwell exhibits a sharp contrast with respect to both emissivity and planetary radius (derived from altimetry) compared to other geologic features, consistent with previous studies. However, the μ_C-only trends does not completely explain the high radar backscatter and associated scattering properties from the Maxwell region. The σ_{OC} - σ_{SC} trends have been suggested as a better diagnostic tool [e.g., 7, 8], and we compared the σ_{OC} - σ_{SC} relations for regions within the Maxwell as well as for Maxwell and other features as shown in Figures 2 and 3 respectively. In both these figures, we observe that there is a positive linear relationship between σ_{OC} and σ_{SC}, and as per [7], the slopes and intercepts derived by a linear least-squares fit (shown here with 1-sigma uncertainty, i.e., variance around the linear fit) constrain the abundance of wavelength-scale particles and effective dielectric permittivity respectively.

Backscatter trends: We infer from Figure 2 that: (i) The radar-bright regions (Maxwell 1, 4) outside of the lower-SC return region as observed by [5] have relatively larger trend line slopes and smaller intercepts (with Maxwell 4 region having a large variance) implying a greater surface rock population and lower effective electric permittivity, likely due to greater porosity; (ii) Lower SC-return regions proximal to the Cleopatra crater (Maxwell 5) and toward its west (Maxwell 3) have similar trend line slopes with little difference in the intercepts implying a rock population with similar size, shape distributions and dielectric properties. (iii) Regions toward south of Cleopatra crater (Maxwell 6) has a higher trend line intercept suggesting a higher effective dielectric permittivity. From figure 3, we suggest that there is a sharp contrast in the near-surface size-density distribution of wavelength-scale scatterers, particle shapes, and material (via permittivity) between Maxwell Montes and other landforms analyzed in this work.

References: [1] Ford P.G. & Pettengill G.H. (1983) *Science* 220, 1379–1381. [2] Pettengill G.H. et al. (1992) *JGR* 97, 13091–13102. [3] Campbell B. et al.

(1999) *JGR* 104, 1897–1916. [4] Treiman A.H. et al. (2016) *Icarus* 280, 172–182. [5] Campbell B.A. & Whitten J.L. (2022) *GRL* 49, 10.1029/2021GL096446. [6] Campbell B.A. & Campbell D.B. (2022) *Planet. Sci. Journal* 3:55, 10.3847/PSJ/ac4f43. [7] Virkki A.K. & Bhiravarasu S.S. (2019) *JGR* 124, 3025–3040. [8] Rivera-Valentín E.G. et al. (2022) *Planet. Sci. Journal* 3:62, 10.3847/PSJ/ac54a0.

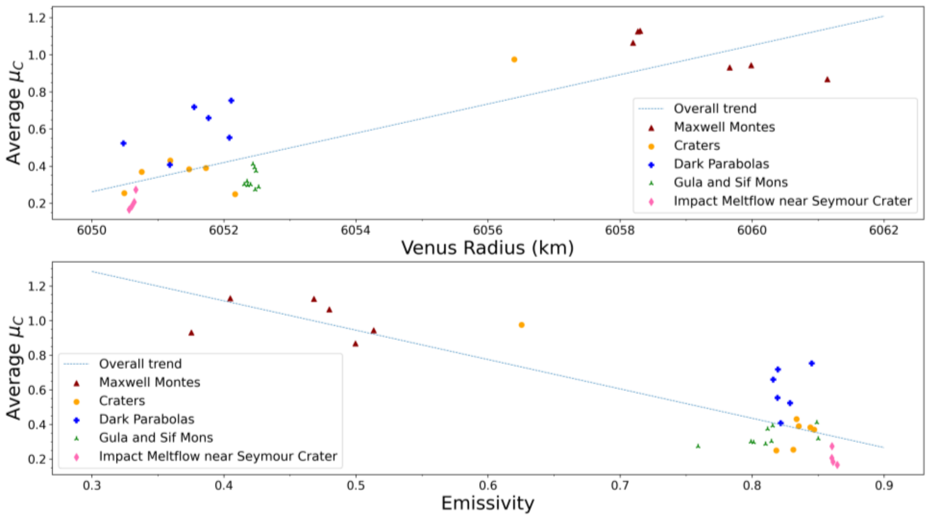

Figure 1: Arecibo S-band Circular Polarization Ratio (μ_C) trends with Venus radius (top) and Emissivity (below) for the features analyzed in this study. Regions from Maxwell Montes (red triangles) could be distinctly identified from the rest of the features

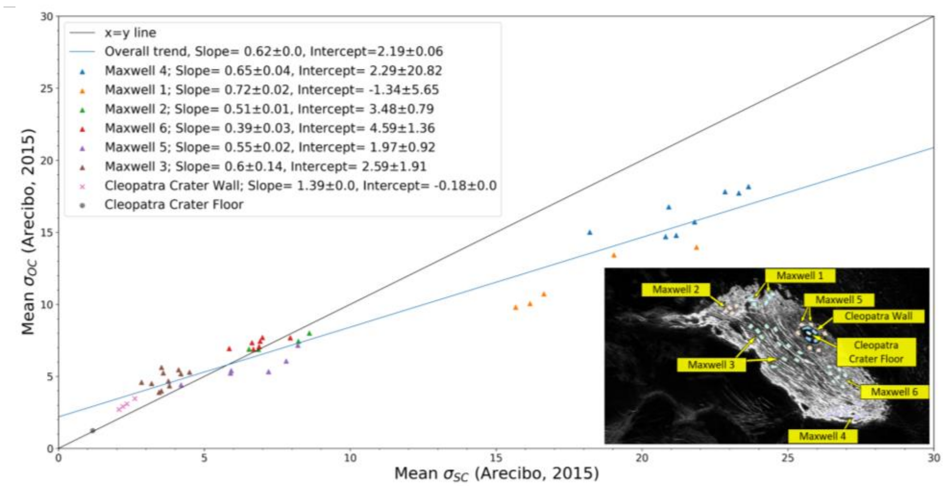

Figure 2: The mean of σ_{OC} plotted against that of σ_{SC} for regions selected from Maxwell Montes, with the solid black and blue lines showing $\sigma_{OC} = \sigma_{SC}$ and the linear least square fit trend, respectively

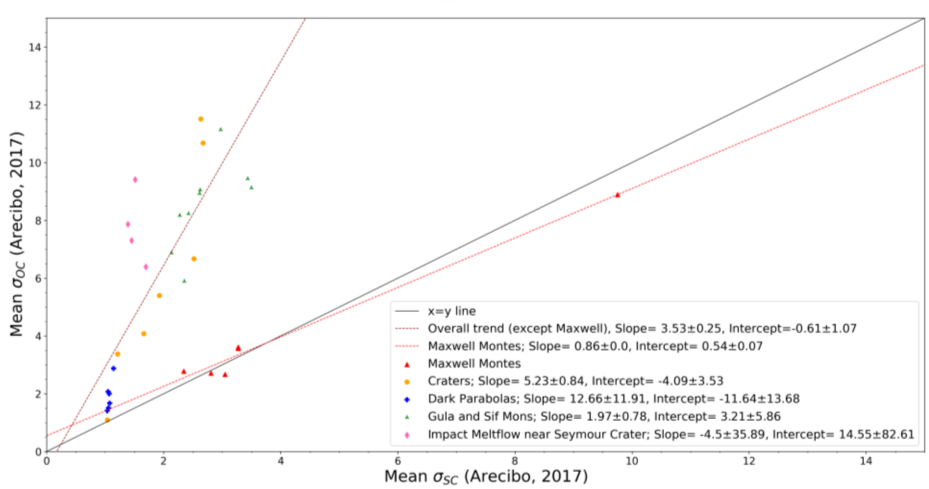

Figure 3: The mean of σ_{OC} plotted against that of σ_{SC} for all regions analyzed in this work. The dark-red dotted line on the left and red dashed line on the right show the linear least square fit trends for *all regions excluding Maxwell* and *only Maxwell region*, respectively. The solid black line shows $\sigma_{OC} = \sigma_{SC}$